EXPERIMENTAL ANALYSIS OF THE INFLUENCE OF AIR FLOW RATE ON WHEAT STRAW COMBUSTION IN A FIXED BED

Zoran M. ČEPIĆ [1], Branka B. NAKOMČIĆ-SMARAGDAKIS [1]*

[1]University of Novi Sad, Faculty of Technical Sciences, Novi Sad, Serbia

* Corresponding author; e-mail: nakomcic@uns.ac.rs

Biomass in the form of crop residues represents a significant energy source in regions whose development is based on agricultural production. Among many possibilities of utilizing biomass for energy generation, combustion is the most common. With the aim of improving and optimizing the combustion process of crop residues, an experimental rig for straw combustion in a fixed bed was constructed. This paper gives a brief review of working characteristics of the experimental rig, as well as the results for three different measuring regimes, with the purpose to investigate the effect of air flow rate on the wheat straw combustion in a fixed bed. For all three regimes analysed in this paper bulk density of the bed was the same - 60 [kgm^{-3}], combustion air was without preheating and air flow rates were: 1152, 1872 and 2124 [kgm^{-2}h^{-1}]. The effect of air flow rate on the ignition rate, burning rate, temperature profile of the bed and flue gas composition were analysed. It was concluded that in the regime with the lowest air flow rate progress of combustion had two clearly conspicuous stages: the ignition propagation stage and the char and unburned material oxidation stage. At the highest air flow rate the entire combustion occurred mostly in a single stage, due to increased air supply oxidized the char, remaining above the ignition front, simultaneously with the reactions of volatiles. Despite that, the optimal combustion process, the highest value of ignition rate, burning rate and bed temperature was achieved with air flow rate of 1872 [kgm^{-2}h^{-1}].

Key words: *biomass, wheat straw, combustion, fixed bed, air flow rate*

1. Introduction

Today's society is facing a dual challenge: the problem of energy shortage and energy security on one hand, and environmental pollution and climate change on the other. Renewable energy sources have the potential to meet both these requirements, more specifically, to enable reliable energy supply while simultaneously reducing the negative impact of energy industry on the environment.

Biomass, which is considered as a renewable energy source, is a power source with the longest tradition of use [1], and it has the potential to become one of the major global primary energy sources of the 21st century [2]. Bio-energy is currently the primary energy source for almost 2.7 billion people worldwide [3]. According to the IEA (International Energy Agency), the total global consumption of biomass and waste energy has increased from 617 Mtoe in 1973 to about 1311 Mtoe in 2011 [4]. Biomass energy accounts for about 15% of the world's primary energy consumption and about 38% of the primary energy consumption in the developing countries. Furthermore, biomass energy

consumption constitutes more than 90% of the total rural energy supplies in developing countries [5]. Recognizing the role of the biomass, many developing countries plan to use its potential for achieving sustainable development. But, the share of biomass is also at high level in the developed countries, so for example in EU the contribution of biomass in the primary production from renewable energy sources is 64% [1, 6].

The demand for biomass in the EU and world-wide is increasing, both in the heating and in the power sector. In 2013, renewable sources generated 26% of EU's electricity, and the target is to reach at least 34% of power generation in 2020 and 45% in 2030. Biomass use for electricity grew by 11% per year during period 2005-2012, and it increased further to reach 18.7% of final renewable electricity consumption in 2013. Power produced from biomass is expected to exceed 839 PJ by 2020 [7].

While future sustainable biomass potentials have been studied in many papers [8-11], in heating and cooling sector biomass is expected to cover 50% of the total contribution from renewable sources, assuming an increase of about 84×10^7 GJ from 2010 to 2020 [12].

In [13] Werther et al. state that on a global level residues from forest-related activities (excluding wood fuel) account for 65% of the biomass energy potential, whereas 33% comes from residues of agricultural crops. Jiang et al. [14] and Liu et al. [15] assert that crop residues are the most commonly considered biomass type.

According to the Intergovernmental Panel on Climate Change (IPCC) biomass energy deployment scenarios, agricultural residues are likely to play an important role in future energy systems contributing between 15 and 70 EJ to long term global energy supply [16]. Agricultural residues are considered to be less contentious, low cost, carry few risks and thus represent an important energy resource for countries with a large agricultural production base [17].

Furthermore, agricultural biomass residues are an attractive alternative to fossil fuels, because of its neutral CO_2 emissions [18]. Another advantage of crop residue is that it is usually free and available in sufficient quantities for self-sustainable heat/hot water supply of a farm/household [13]. This way the higher cost of equipment for biomass combustion could be partially offset by cost-free fuel.

Although large quantities of agricultural residues are generated each year, the current level of their utilization as fuel is still relatively low. Lack of sufficient information concerning fuel feeding and the combustion characteristics, as well as ash content and pollutant emissions of these residues are reasons for the current low level of utilization of agricultural residues [13, 19].

In whatever form agricultural residues are burned (loose, baled, briquettes, pellets), a more profound understanding of the combustion mechanisms is necessary in order to achieve a high combustion efficiency and to effectively design and operate the combustion systems.

The interconnected events through which single particles of solid fuel go during combustion are heating up, drying, devolatilization and finally the combustion of the volatiles and char. The temperatures at which devolatilization and char combustion start, the influence of drying on the devolatilization process, the composition of the devolatilization products and the effect of volatile release and combustion on the overall combustion process, are all significant information required to understand the combustion characteristics of agricultural residues [13].

The method of burning is one of the defining factors that influence the quality of combustion and gaseous and particulate emissions from the use of agricultural residues. Fixed-bed combustion in

both small- and large-scale grate furnaces (domestic boilers, stoves, district heating plants) is a suitable and common method to transform solid biomass into thermal energy [20, 21].

There has been some research during the last two decades; however, more detailed research is needed to increase the understanding of the biomass fixed bed combustion processes. In two earlier papers, Horttanainen et al. [22] and Saastamoinen et al. [23], concerning operational limits of ignition front propagation against airflow in packed beds of different wood fuels. Porteiro et al. in his paper [24] described an experimental analysis of the ignition front propagation of several biomasses in a mainly one-dimensional fixed-bed combustor. The propagation of a reaction front through a fixed bed was theoretically analysed by Gort [25]. The results can be applied to any fixed bed conversion process where a reaction front is formed that moves in opposite direction to the flow of the gaseous reactant. Thunman and Leckner in [26] have developed a generalized model for combustion of solid biofuel in a fixed bed on a grate. The model can be applied to co-current and counter-current combustion of any solid biofuel, and the results show how the different phases, drying, devolatilization and char combustion interact during conversion.

Biomass and particularity straw combustion has been researched in several papers. Van der Lans [27] developed a two-dimensional mathematical model for straw combustion in a cross-current moving bed. To verify the model and to increase the understanding of straw bed combustion process, experimental investigation with variation of primary air flow rate and air preheat temperature was conducted. His work was extended by Zhou [28] who developed a one-dimensional model of fixed-bed straw combustion and validated the results with the experimental measurements of temperature, gas emissions, ignition front propagation rate and flame temperature. Miljkovic [29] investigated wheat straw combustion in fixed bed combustor. Her work was focused on defining mass loss rate as a function of time for different combinations of bulk density and air flow velocity.

During combustion process, oxygen deficiency leads to incomplete combustion and the formation of many products of incomplete combustion. Excess air cools the system. The air requirements depend on the chemical and physical characteristics of the fuel, as well as bed density. The combustion of the biomass relates to the fuel burn rate, the combustion products, the required excess air for complete combustion, and the fire temperatures [30]. Emissions from incomplete combustion reflect the chemical composition of the fuel and indicate the compounds that can be emitted during, e.g., start-ups and temporary disturbances [31].

The crucial combustion parameter, primary air flow rate, has been extensively studied by researchers such as Yang [32], Khor [33], Wiinikka and Gebart [20], Rogame [34], Janic [35] and others.

Yang in his paper [32] investigated primary air flow as a major controlling parameter to maintain the stability of the combustion and achieve the desired burning rate, temperature and gas composition. In [33] Khor et al. investigated in a fixed-bed reactor for a range of air flow-rates. Measured temperatures, gas composition and mass loss were used to evaluate the combustion characteristics in terms of ignition front speed, burning rate, percentage of mass loss and the equivalence ratio. The average burning rates of herbaceous fuels reached a peak of 220-250 [$kgm^{-2}h^{-1}$] at air flow rates of 700-900 [$kgm^{-2}h^{-1}$]. An overlap of the two distinct periods of combustion was observed at high air flow rates, as the air supply was sufficient to simultaneously burn the char above the ignition front. When uncut straw was burned, less uniform packing of the long fibres increased the effect of air channelling and led to irregular propagation of the ignition front. Furthermore, in [20]

Wiinikka and Gebart investigated biomass combustion in fixed bed and the influence of air distribution rate on particle emissions. Results have shown that the air supply affects the emissions of both coarse and especially fine fly ash particles and that changing or optimizing the air supply strategy appears to be an attractive way to reduce the particle emissions already in the combustion process. The importance of air distribution rate has been moreover researched by Rogaume et al. in [34]. In this paper an experimental study was conducted and carbon monoxide, nitrogen oxide and temperature measurements have been used to establish the importance of the operating parameters of a municipal waste incinerator in the characteristics of the combustion process. Results showed that air distribution rate is an important parameter when optimizing combustion process and that varying primary and secondary air rates/amounts significantly influences emissions and combustion quality. Janic in his paper [35] investigated correlation between thermal power output and the quantity and composition of air for the combustion of soybean straw bales in hot water boiler plant with flat, fixed, and water-cooled grate.

This paper presents an experimental investigation into the combustion behaviour of wheat straw in a fixed bed. The effects of primary air flow rate are analysed. This work focuses on improving the understanding of this fuel to obtain data on the reaction front propagation rate, temperature distribution inside the bed and composition of the flue gases.

2. Materials and method

2.1. Experimental rig

Figure 1 shows a schematic diagram of the experimental rig. The rig consists of a vertical cylindrical combustion chamber, height of 1080 mm and inside diameter of 230 mm, as it has been described in the paper [29]. The chamber is made from chromium sheet steel 2 mm thick, coated with 50 mm thick ceramic wool, covered by a thick layer of external casing. At the bottom of the reactor is a steel grate through which the fan blows the combustion air. An electrical radiation heater was used in order to ignite the fuel. Ni/Cr-thermocouples (type K) were used to measure the bed temperature at different heights. A gas sampling probe was placed in the chimney at 1000 mm above the reactor (or 2080 mm above the great) and connected to a gas analyser for continuously measuring of CO, CO_2 and O_2. The entire reactor is placed on the weighing scale.

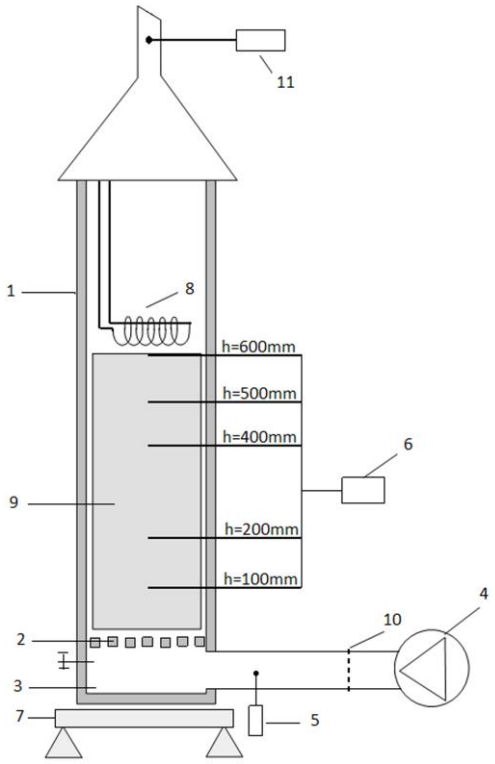

Figure 1. Schematic diagram of the experimental rig

Experimental rig elements: 1- reactor, 2- grate, 3- ashtray, 4- air fan, 5- air flow meter, 6- thermocouples with data logger, 7- weighing scale, 8- electric heater, 9- wheat straw (Ø230 x 600 mm), 10- air flow laminator, 11- gas analyser.

2.2. Sample preparation and experimental conditions

Wheat straw, used in the experiment, was left in a field at high temperatures about seven days after harvest and then baled in the form of standard bale dimensions 0.4 × 0.5 × 1 m. Weight of bales was around 12 kg, i.e. 60 [kgm^{-3}], so the straw stems were not damaged. Straw used in the experiment, was carefully taken from randomly selected bales, without any previous preparation (cutting or rolling). Properties of the wheat straw are listed in tab. 1.

Table 1: Wheat straw properties

Moisture [wt%]	Volatile [wt%]	Fixed carbon [wt%]	Ash [wt%]	Higher heating value [MJ]
9.2	71.7	9.8	9.3	16.7

The reactor was filled with wheat straw to a height of 600 mm, measured from the grate. Special attention was dedicated to achieving a uniform bulk density of the bed, which was 60 [kgm^{-3}], as in the origin bales. Electric start-up heater is placed inside the reactor at 5-10 mm above the bed. When the straw ignites, the electric heater is turned off, the air fan is turned on, and counter-current combustion is established. By regulating the fan speed it is possible to achieve different conditions of combustion and/or pyrolysis. The experiments were carried out with three air flow rates: 1152 [$kgm^{-2}h^{-1}$] (Case WS1), 1872 [$kgm^{-2}h^{-1}$] (Case WS2) and 2124 [$kgm^{-2}h^{-1}$] (Case WS3). Five thermocouples, placed at

the vertical axis of the reactor at 100, 200, 400, 500, and 600 mm measured from the grate, were employed to determine ignition and propagation of a reaction front in the bed, as well as temperature distribution inside the bed. By placing the entire reactor on the weighing scale it was possible to monitor mass loss history.

3. Results and discussion

3.1. Mass loss history

Combustion of wheat straw in a fixed bed may be divided into four consecutive or overlapping sub-processes: evaporation of moisture from straw, volatile release – char formation, combustion of the volatiles and the oxidation of char particles. Once the straw is ignited by an external heat source (electrical radiation heater), the ignition front propagates into the bed, marking the beginning of ignition propagation stage. The heat, generated in the reaction front, is transported against the flow of combustion air and dries and devolatilises the raw straw. Due to opposite directions of heat and air flow, the heat is not transported downwards far from the reaction zone and hence the reaction front stays very thin during the ignition propagation stage [29, 36]. Since the heterogeneous char oxidation is relatively slow and oxygen is consumed first by the volatile gases from the particles, carbonised particles remain above the ignition front. Therefore, the drying, volatile release/char formation, combustion of the volatiles, char oxidation and ash zones appear sequentially from the bottom to the top of the bed during the ignition propagation, although these processes occur simultaneously. Once the ignition front reaches the bottom of the bed, ignition propagation stage is ended and begins char oxidation stage.

Two process rates are often used to quantify the progress of straw combustion in fixed bed – burning rate and ignition rate. The burning rate ($kgm^{-2}h^{-1}$) can be defined as the mass deficit of straw over time, normalized by the cross-sectional area of the bed. The most common method of determining the burning rate is by employing a weighing scale to measure mass loss (with time). Although the ignition rate has the same units as the burning rate ($kgm^{-2}h^{-1}$), it is derived differently. The ignition rate is the rate of mass per unit cross-sectional area through which the ignition front passed. It was calculated by multiplying the ignition front speed by the bulk density of the bed. The ignition front speed can be derived from the experimental data from the distance between the thermocouples and the time for the ignition front to travel between two thermocouples [4, 21, 24, 33, 37-39].

As the material should be pyrolysed before combustion, the ignition rate is always higher than the burning rate. The difference between the ignition rate and burning rate is the rate of mass accumulated above the ignition front, which is char and, if any, fresh material. As the remaining material after the ignition propagation stage burns at a much lower burning rate, it is desirable to minimize the duration of the char oxidation stage by increasing the mass loss in the ignition propagation stage [33].

The difference between characterizing bed performance using either burning rate or ignition rate becomes more obvious at lower air flow rates. In a lower air flow rate regime, steady state conditions are harder to reach, therefore burning rate is significantly lower than ignition rate as a result of unburned char and ash accumulating over the ignition front [4, 33, 36, 38, 39].

Figure 2 shows the mass loss history of wheat straw expressed as a percentage of the remaining mass on the bed. For all three cases, during the ignition propagation period, the mass left on the bed decreases with a uniform slope. The gradient of the curves increased as the air flow rate increased, from the air flow rate of 1152 [$kgm^{-2}h^{-1}$] for Case WS1 to 1872 [$kgm^{-2}h^{-1}$] for Case WS2, and then decreased at air flow rate of 2124 [$kgm^{-2}h^{-1}$] for Case WS3.

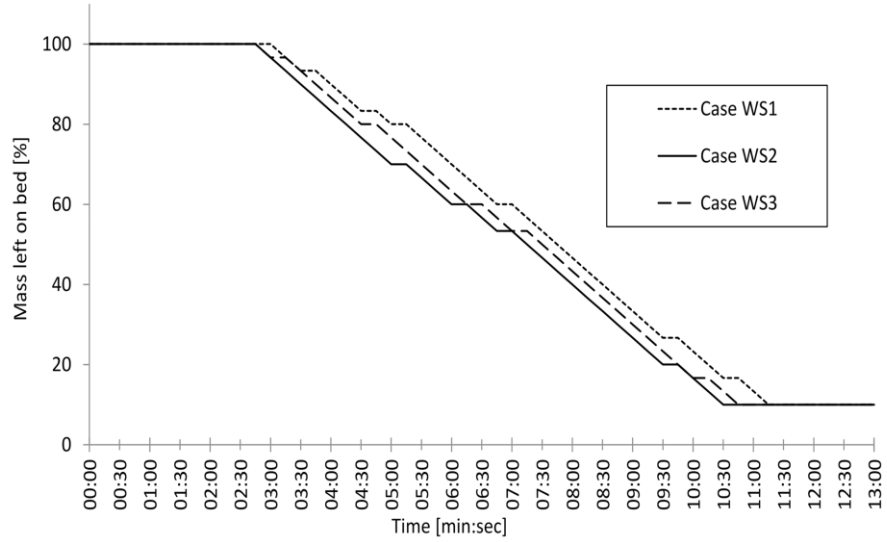

Figure 2. Mass loss history as a function of reaction time

At the end of the ignition propagation stage (steady mass loss period), the mass loss slowed down gradually which indicates the second stage of combustion (char oxidation stage). Case WS3 had the shortest char oxidation stage (around 45 seconds), but burning rate wasn't the highest (248 [$kgm^{-2}h^{-1}$]) as a consequence of overcooling. For the case of straw combustion at the lowest air flow rate (Case WS1), the ignition rate was much higher than the burning rate, as a consequence of insufficient combustion air (see tab. 2). The optimal air flow rate was around 1872 [$kgm^{-2}h^{-1}$] (Case WS2) which provided a maximum burning rate (257 [$kgm^{-2}h^{-1}$]), slightly higher ignition rate (260 [$kgm^{-2}h^{-1}$]) and short char oxidation stage (less than a minute). Furthermore, in this case, the mass loss in the ignition propagation stage was about 80%. It suggests that all the fuel was pyrolysed and some of the char produced was oxidised during the ignition propagation stage.

Table 2. Key parameters of combustion for wheat straw

Case	Bulk density [kgm^{-3}]	Air flow rate [$kgm^{-2}h^{-1}$]	Mass loss in ignition propagation stage [%]	Ignition front speed [m/h]	Ignition rate [$kgm^{-2}h^{-1}$]	Burning rate [$kgm^{-2}h^{-1}$]	Air excess ratio [-]
WS1	60	1152	73	4.75	285	243	1.0
WS2	60	1872	80	4.33	260	257	1.5
WS3	60	2124	83	4.17	250	248	1.8

3.2. Bed temperature profile and gas composition

Figures 3a, 4a and 5a show the measured temperature history at different bed heights for all three cases. As already mentioned, two stages of combustion can be clearly identified in the

temperature curves. In the ignition propagation stage, the local bed temperature increased sharply from room level to a peak value (850-1200 °C) and then dropped as the ignition front propagates down the bed, but still remains relatively high because of the hot gases from the reaction front downstream of the thermocouple. The average time interval required for each temperature jump in ignition propagation stage was less than 1 min.

After the propagation of the ignition front, temperatures on all thermocouples in the bed began to rise simultaneously and reached a peak at around t = 11, 10:30 and 10:15 min, respectively for cases WS1, WS2 and WS3. In all three cases, peak temperatures appeared in the zone of the lowest thermocouple which suggests active combustion at the bottom of the bed. Such a temperature increase can be explained in the following way. The main oxidation zone, in char oxidation stage, stays in the lower part of the bed, where the oxygen is consumed by char and/or unburned straw. The heat generated in the char oxidation stage is transferred upward by radiation and convection with gas. Also, char is carbon rich fuel and therefore can increase the bed temperature much more than straw combusted in the ignition propagation stage. The gradual decrease in temperatures marked the end of the combustion.

Another important parameter which can be used to describe combustion efficiency is peak temperature. The peak temperature responds to an increasing of the air flow rate, in the way, it will rise until a critical air flow rate is reached. Beyond this value, the peak temperature will remain at a relatively constant level, or even slightly fall down.

In Case WS1, due to the high fuel-rich conditions, the peak temperatures recorded in the ignition propagation stage were 860-1050 °C, and in the char oxidation stage were about 960 °C. At high air flow rates, the char oxidation stage was shorter with recorded temperature peaks about 1050 and 1030 °C for Case WS2 and WS3, respectively. In both these cases the peak temperatures in the ignition propagation stage rose sharply to over 1000 °C, even up to 1200 °C.

Gas compositions are important in that they provide information of further reactions needed in the over-bed zone to complete the combustion. Figures 3b, 4b and 5b show the measured gas concentration at the probe position of 2080 mm above the grate.

In the Case WS1 (fig. 3b) O_2 concentration drops rapidly from 21 to less than 1%, while simultaneously CO and CO_2 rise sharply from 0% to about 4 and 5%, respectively. During ignition propagation stage level of CO_2 was around 5%, but it is interesting to note increase of CO_2 concentration between t = 9 and 12 min, that comes from char oxidation in char oxidation stage, which has already been discussed. The high concentration of CO was due to the fuel-rich conditions, but as the rate of mass loss gradually decreased, CO concentration declined steadily from 4% to less than 1%. O_2 concentration began to rise at t = 10 min marking the final combustion stage.

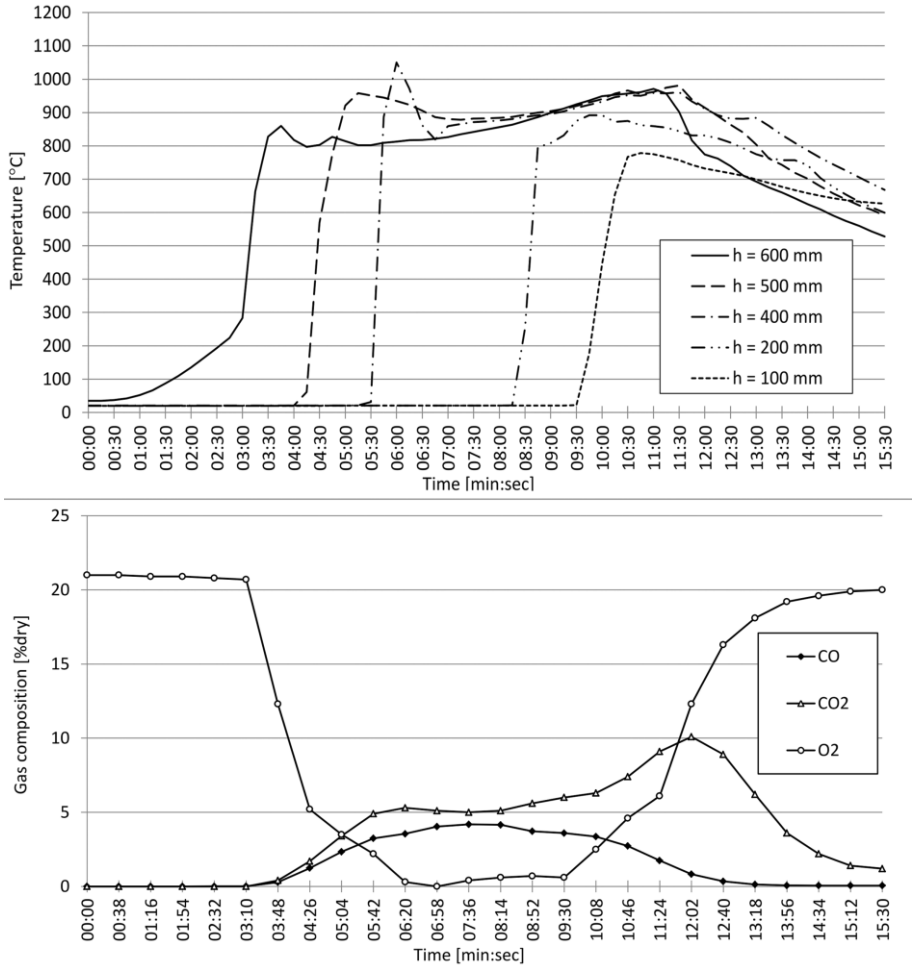

Figure 3. Bed temperature profile (a) and gas composition (b) for Case WS1

The O_2 concentration in the Case WS2 (fig. 4b) quickly dropped from the ambient level to about 6%, as soon as the ignition front propagated downwards, and stayed relatively steady until finial char combustion reaction. After the initial rise of CO (peak value was about 1,3%), it quickly started to decrease and stayed below 0,4% for the rest of the combustion. CO_2 diagram shows slight char oxidation in final stage of combustion, until it drops off marking the end of combustion.

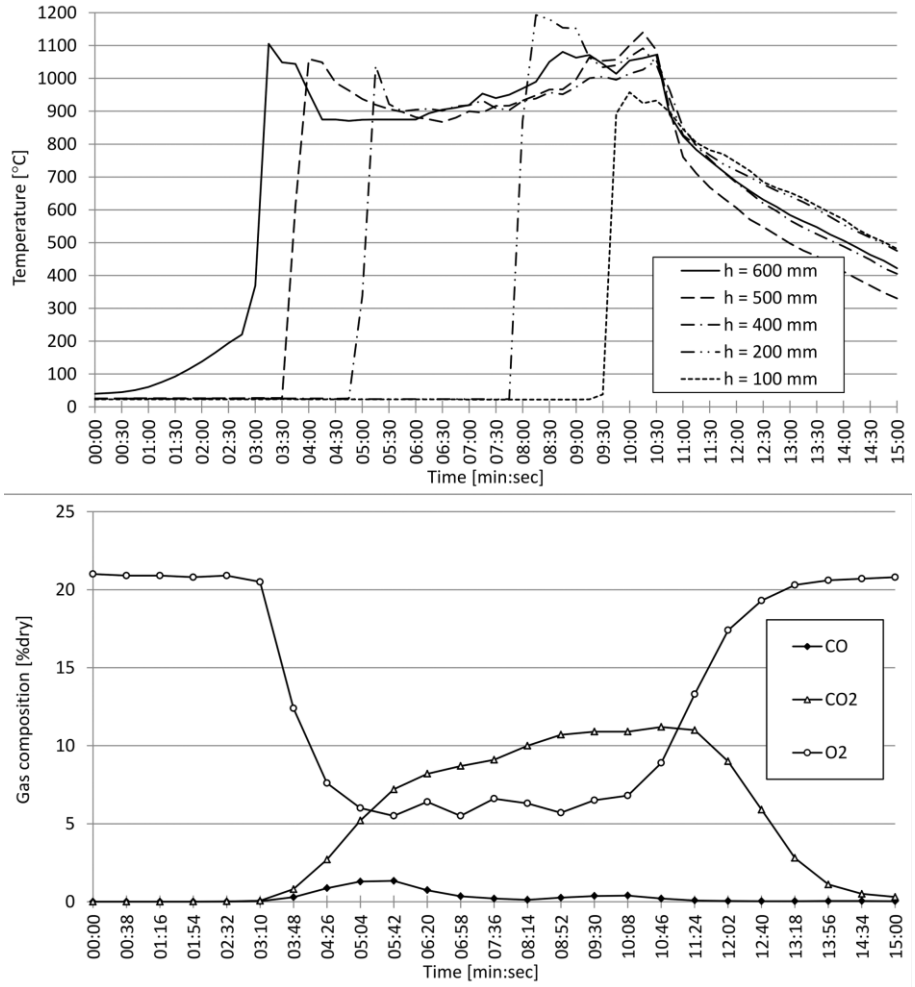

Figure 4. Bed temperature profile (a) and gas composition (b) for Case WS2

In the Case WS3 (fig. 5b) O_2 concentration dropped quickly in less than a minute from 21% to 10%, marking the beginning of combustion process. Simultaneously, the concentrations of CO and CO_2 have started to rise. The CO concentration showed a slight growing trend only at the beginning of the combustion, but it was still below 1%, while the rest of the combustion had a value close to zero. During ignition propagation stage, the concentration of CO_2 in the flue gas was just below 10%, but a slight increase is noticeable in the final stages of combustion (char oxidation stage), indicating a burning of a small amount of the unburned char. The end point of combustion was determined by the increase in oxygen concentration.

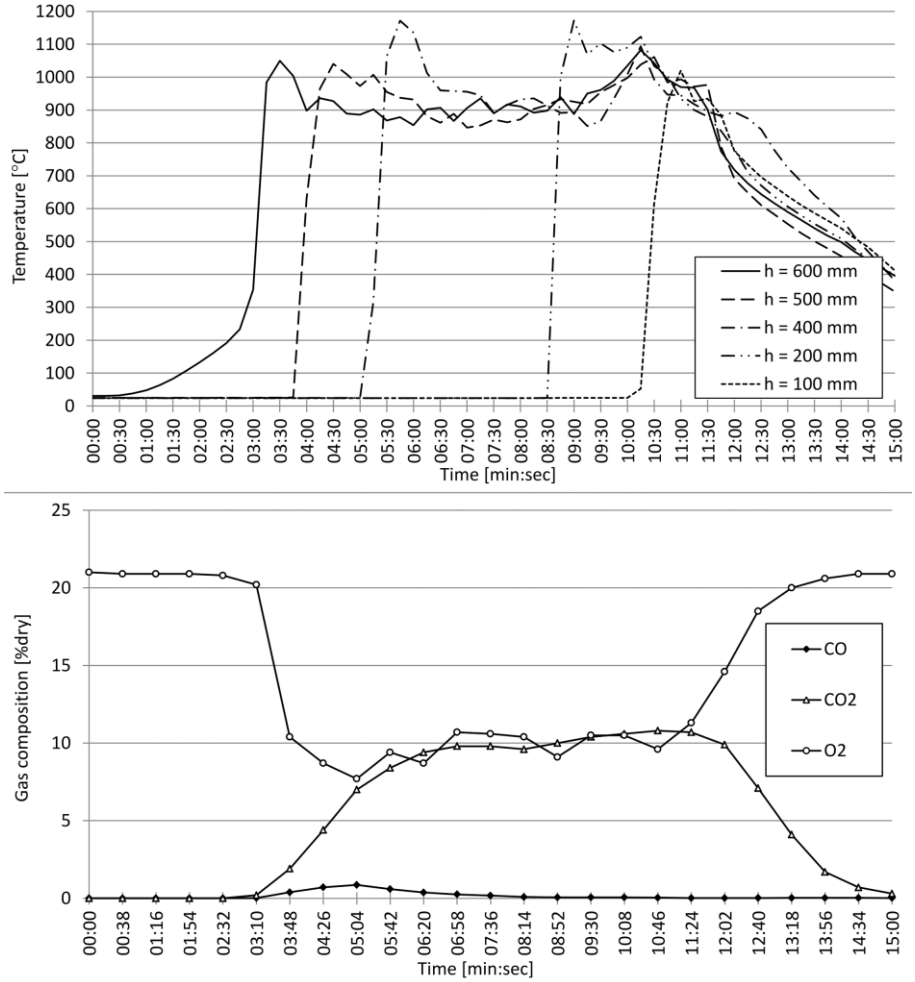

Figure 5. Bed temperature profile (a) and gas composition (b) for Case WS3

4. Conclusion

This paper presents an experimental investigation of the wheat straw combustion in a fixed bed. Primary air flow is employed as a major combustion controlling parameter and his effects on ignition and burning rate, temperature distribution inside the bed and flue gas composition were analysed. Experiments were conducted for three different air flow rates, 1152 [$kgm^{-2}h^{-1}$] (Case WS1), 1872 [$kgm^{-2}h^{-1}$] (Case WS2) and 2124 [$kgm^{-2}h^{-1}$] (Case WS3).

Temperature, gas composition and mass loss curves identified two distinct periods as the combustion progresses in the bed: the ignition propagation and char oxidation.

At low air flow rate (Case WS1), the progress of combustion had two clearly conspicuous stages: the ignition propagation stage and the char and unburned material oxidation stage. At high air flow rate (Case WS3) the whole combustion occurred mostly in a single stage, due to increased air supply oxidized the char remaining above the ignition front simultaneously with the reactions of volatiles. Despite that, the optimal combustion process, the highest value of ignition rate, burning rate and bed temperature was achieved in Case WS2.

It is found that the burning rate increases with an increase in the primary air flow, until a critical point is reached, where a further increase in the air flow results in a fall in the burning rate. The critical air flow rate reflects the balance between the heat absorbed by the solid particles and the heat loss to

the cooler gas stream from the particles. Also, high primary air flow reduces the char fraction burned in the final char oxidation stage, shifts combustion in the bed to a more fuel lean environment and reduces CO emission.

It should be emphases that in Case WS2 although around 6% of oxygen was present in the flue gas throughout the entire ignition propagation stage, small amount of unburned char was left after this stage was finished. This indicates that the consumption of oxygen in the bed was not efficient enough and points to the need of changing the method of delivering the combustion air.

Increasing the combustion efficiency could be achieved by delivering the air in two ways: as a primary air flow rate (through the grate) and as a secondary air flow rate (at the top of the bed). These are also the recommendations for future investigation and research of wheat straw combustion in a fixed bed.

5. References

[1] Kanevce, G., *et al*., Optimal Usage of Biomass for Energy Purposes Toward Sustainable Development - A Case of Macedonia, *Thermal Science, 20* (2016), Suppl. 1, pp. S77-S91.

[2] Dhillon, R.S., von Wuehlisch, G., Mitigation of Global Warming through Renewable Biomass, *Biomass and Bioenergy, 48* (2013), pp. 75-89.

[3] Bildirici, M., Özaksoy, F., Woody Biomass Energy Consumption and Economic Growth in Sub-Saharan Africa, *Procedia Economics and Finance, 38* (2016), pp. 287-293.

[4] Khodaei, H., *et al.*, An overview of processes and considerations in the modelling of fixed-bed biomass combustion, *Energy, 88* (2015), pp. 946-972.

[5] Bildirici, M., Özaksoy, F., The Relationship Between Economic Growth and Biomass Energy Consumption in some European Countries, *Journal of Renewable and Sustainable Energy, 5* (2013), DOI: http://dx.doi.org/10.1063/1.4802944

[6] Turanjanin, V., *et al*., Development of the Boiler for Combustion of Agricultural Biomass by Products, *Thermal Science, 14* (2010), 3, pp. 707-714.

[7] Giuntoli, J., *et al*., Climate change impacts of power generation from residual biomass, *Biomass and Bioenergy, 89* (2016), pp. 146-158.

[8] Thrän, D., *et al*., Global Biomass Potentials – Resources, Drivers and Scenario Results, *Energy for Sustainable Development, 14* (2010), 3, pp. 200-205.

[9] Durusoy, I., et al., Sustainable Agriculture and the Production of Biomass for Energy Use, *Energy Sources, Part A: Recovery, Utilization, And Environmental Effects, 33* (2011), 10, pp. 938-947.

[10] Radovanović, P., *et al*., Opportunities of Solid Renewable Fuels for (Co-) Combustion with Coal in Power Plants in Serbia, *Thermal Science, 18* (2014), 2, pp. 631-644.

[11] Alidrisi, H., and Demirbas, A., Enhanced electricity generation using biomass materials, *Energy Sources, Part A: Recovery, Utilization, And Environmental Effects, 38* (2016) , 10, pp. 1419-1427.

[12] Granada, E., *et al*., Experimental Analysis of Several Biomass Fuels: The Effect of the Devolatilization Rate on Packed Bed Combustion, *Journal of Renewable and Sustainable Energy, 4* (2012), DOI: http://dx.doi.org/10.1063/1.4738593

[13] Werther, J., *et al*., Combustion of Agricultural Residues, *Progress in Energy and Combustion Science, 26* (2000), pp. 1-27.

[14] Jiang, D., *et al*., Bioenergy Potential from Crop Residues in China: Availability and Distribution, *Renewable and Sustainable Energy Reviews, 16* (2012), 3, pp. 1377-1382.
[15] Liu, J., *et al*., Quantitative Assessment of Bioenergy from Crop Stalk Resources in Inner Mongolia, China, *Applied Energy, 93* (2012), pp. 305-318.
[16] Batidzirai, B., *et al*., Current and future technical, economic and environmental feasibility of maize and wheat residues supply for biomass energy application: Illustrated for South Africa, *Biomass and Bioenergy, 92* (2016), pp. 106-129.
[17] Dornburg, V., *et al*., Bioenergy revisited: Key factors in global potentials of bioenergy, *Energy & Environmental Science, 3* (2010), pp. 258-267.
[18] Urosevic, D., Gvozdenac-Urosevic, B., Comprehensive Analysis of a Straw-Fired Power Plant in Vojvodina, *Thermal Science, 16* (2012), Suppl. 1, pp. S97-S106.
[19] Kaygusuz, K., Biomass as a Renewable Energy Source for Sustainable Fuels, *Energy Sources, Part A: Recovery, Utilization, and Environmental Effects, 31* (2009), 6, pp. 535-545.
[20] Wiinikka, H., Gebart, R., The Influence of Air Distribution Rate on Particle Emissions in Fixed Bed Combustion of Biomass, *Combustion Science and Technology, 177* (2005), 9, pp. 1747-1766.
[21] Porteiro, J., *et al*., Study of a Fixed-Bed Biomass Combustor: Influential Parameters on Ignition Front Propagation Using Parametric Analysis, *Energy Fuels, 24* (2010), 7, pp. 3890-3897.
[22] Horttanainen, M., *et al*., Operational Limits of Ignition Front Propagation against Airflow in Packed Beds of Different Wood Fuels, *Energy & Fuels, 16* (2002), 3, pp. 676-686.
[23] Saastamoinen, J. J., *et al*., Propagation of the Ignition Front in Beds of Wood Particles, *Combustion and Flame,123* (2000), 1-2, pp. 214-226.
[24] Porteiro, J., *et al*., Experimental Analysis of the Ignition Front Propagation of Several Biomass Fuels in a Fixed-Bed Combustor, *Fuel, 89* (2010), 1, pp. 26-35.
[25] Gort, R., Brouwers, J.J.H., Theoretical Analysis of the Propagation of a Reaction Front in a Packed Bed, *Combustion and Flame, 124* (2001), 1–2, pp. 1-13.
[26] Thunman, H., Leckner, B., Co-Current and Counter-Current Fixed Bed Combustion of Biofuel – A Comparison, *Fuel, 82* (2003), 3, pp. 275-283.
[27] Van der Lans, R.P., *et al*., Modelling and Experiments of Straw Combustion in a Grate Furnace, *Biomass and Bioenergy, 19* (2000), pp. 199-208.
[28] Zhou, H., *et al*., Numerical Modeling of Straw Combustion in a Fixed Bed, *Fuel, 84* (2005), pp. 389-403.
[29] Miljkovic, B., Experimental Facility for Analysis of Biomass Combustion Characteristics, *Thermal Science, 19* (2015), 1, pp. 341-350.
[30] Demirbas, A., Combustion of Biomass, *Energy Sources, Part A: Recovery, Utilization, and Environmental Effects, 29* (2007), 6, pp. 549-561.
[31] Olsson, M., Wheat Straw and Peat for Fuel Pellets-Organic Compounds from Combustion, *Biomass and Bioenergy, 30* (2006), 6, pp. 555-564.
[32] Yang, Y.B., *et al*., Effect of Air Flow Rate and Fuel Moisture on the Burning Behaviours of Biomass and Simulated Municipal Solid Wastes in Packed Beds, *Fuel, 83* (2004), 11–12, pp. 1553-1562.
[33] Khor, A., *et al*., Straw combustion in a fixed bed combustor, *Fuel, 86* (2007), pp. 152-160.

[34] Rogaume, T., *et al*., The Effects of Different Airflows on the Formation of Pollutants during Waste Incineration, *Fuel, 81* (2002), 17, pp. 2277-2288.
[35] Janic, T., *et al*., Thermal Power of Small Scale Manually Fed Boiler, *Thermal Science, 19* (2015), 1, pp. 329-340.
[36] Porteiro, J., *et al*., Study of the reaction front thickness in a counter-current fixed-bed combustor of a pelletised biomass, *Combustion and Flame, 159* (2012), 3, pp. 1296-1302.
[37] Ryu, C., *et al*., Ignition and burning rates of segregated waste combustion in packed beds, *Waste Management, 27* (2007), 6, pp. 802-810.
[38] Ryu, C., *et al*., Effect of fuel properties on biomass combustion: part I experiments – fuel type, equivalence ratio and particle size, *Fuel, 85* (2006), 7-8, pp. 1039–1046
[39] Zhao, W., *et al*., Effect of air preheating and fuel moisture on combustion characteristics of corn straw in a fixed bed, *Energy Conversion and Management, 49* (2008), 12, pp. 3560-3565.